Divergent Regulation of Energy Expenditure and Hepatic Glucose Production by Insulin Receptor in Agouti-Related Protein and POMC Neurons

Hua V. Lin,[1] Leona Plum,[1] Hiraku Ono,[2] Roger Gutiérrez-Juárez,[2] Marya Shanabrough,[3] Erzsebet Borok,[3] Tamas L. Horvath,[3] Luciano Rossetti,[2] and Domenico Accili[1]

OBJECTIVE—The sites of insulin action in the central nervous system that regulate glucose metabolism and energy expenditure are incompletely characterized. We have shown that mice with hypothalamic deficiency (L1) of insulin receptors (InsRs) fail to regulate hepatic glucose production (HGP) in response to insulin.

RESEARCH DESIGN AND METHODS—To distinguish neurons that mediate insulin's effects on HGP from those that regulate energy homeostasis, we used targeted knock-ins to express InsRs in agouti-related protein (AgRP) or proopiomelanocortin (POMC) neurons of L1 mice.

RESULTS—Restoration of insulin action in AgRP neurons normalized insulin suppression of HGP. Surprisingly, POMC-specific InsR knock-in increased energy expenditure and locomotor activity, exacerbated insulin resistance and increased HGP, associated with decreased expression of the ATP-sensitive K^+ channel (K_{ATP} channel) sulfonylurea receptor 1 subunit, and decreased inhibitory synaptic contacts on POMC neurons.

CONCLUSIONS—The contrasting phenotypes of InsR knock-ins in POMC and AgRP neurons suggest a branched-pathway model of hypothalamic insulin signaling in which InsR signaling in AgRP neurons decreases HGP, whereas InsR activation in POMC neurons promotes HGP and activates the melanocortinergic energy expenditure program. ***Diabetes*** **59:337–346, 2010**

Insulin receptor (InsR) signaling in the central nervous system (1,2) regulates energy balance (3). Inactivation of InsR in neurons and glia ("NIRKO" mice) predisposes to diet-induced obesity (4), whereas intracerebroventricular insulin administration results in acute suppression of food intake (3,5,6) and stimulation of energy expenditure (7). Furthermore, central nervous system insulin signaling regulates glucose metabolism. NIRKO mice show mild insulin resistance (4). And hypothalamic insulin signaling via phosphatidylinositol 3-kinase (PI 3-kinase) and ATP-sensitive K^+ channels (K_{ATP} channels) (8) is required for insulin suppression of hepatic glucose production (HGP) (9,10).

The functional neuroanatomy of InsR signaling has yet to be mapped. Conditional ablation of InsR in agouti-related protein (AgRP) neurons results in altered HGP, whereas proopiomelanocortin (POMC) neuron-specific knockout is conspicuous by its lack of phenotype (11). But unlike leptin receptor signaling, where it has been possible to dissect pathways regulating food intake from those regulating energy expenditure (12) and reproduction (13), the question of which neurons mediate specific actions of insulin remains largely unsettled.

Using a genetic reconstitution approach, we have embarked on a systematic analysis of tissue interactions required to maintain normal insulin sensitivity. Complete ablation of InsR results in lethal neonatal diabetes (14) that, surprisingly, can be rescued by restoring InsR expression in liver, pancreatic β-cells, and several brain regions (L1 mice) (15). L1 mice have a >90% reduction of InsR levels in the hypothalamic arcuate nucleus (ARC) and blunted insulin signaling in hypothalamic cell extracts, associated with impaired regulation of HGP (10). Thus, they can be considered a model of impaired insulin signaling in key hypothalamic cell subpopulations, whose neuropeptide products have profound effects on energy homeostasis (3). To analyze the contribution of these different neuronal cell types to insulin action, we used a gain-of-function approach to reconstitute InsR expression in either AgRP or POMC neurons of L1 mice and analyzed their bioenergetic and metabolic phenotypes.

RESEARCH DESIGN AND METHODS

Mice. *Insr*$^{-/-}$ (14), *Ttr-INSR* transgenic, *βac/INSR* knock-in (15), *Foxo1*$^{flox/flox}$ (16), *Agrp-Cre* (17), and *Pomc-Cre* (18) mice have been previously described. *Insr*$^{+/-}$::*Ttr-INSR*::*βac/INSR* mice were intercrossed with *Agrp-Cre* or *Pomc-Cre* mice to generate *Insr*$^{-/-}$::*Ttr-INSR*::*βac/INSR*::*Agrp-Cre* (Agrp-KI) and *Insr*$^{-/-}$::*Ttr-INSR*::*βac/INSR*::*Pomc-Cre* (Pomc-KI) mice. Wild-type littermates were used as controls. Genotyping was performed as previously described (15,17–19). Embryonic recombination of the *βac/INSR* locus was detected by PCR from tail DNA of an ~200-bp product using primers 5′-GGTTTTCCTTT GAAAAACACG-3′ and 5′-CTTAATCGCCTTGCAGCACAT-3′. *Foxo1*$^{\Delta POMC}$ (*Foxo1*$^{flox/flox}$::*Pomc-Cre*) mice were obtained by mating *Foxo1*$^{flox/flox}$ mice with *Pomc-Cre* mice (18). All animal procedures have been approved by the Columbia University Institutional Animal Care and Utilization Committee.

Metabolic analyses. Metabolites were measured as described (20). Free fatty acids and triglycerides were measured with NEFA-HR test reagents (Wako Chemicals, Richmond, VA) and serum triglyceride determination kit (Sigma, St. Louis, MO). Insulin and leptin were measured by enzyme-linked immunosorbent assay; adiponectin, resistin, tissue plasminogen activator inhibitor 1, interleukin-6 (IL-6), and tumor necrosis factor-α by Luminex (Linco Research, St. Charles, MO); IGF-1 (Alpco Diagnostics, Salem, NH), corticosterone (MP Biomedicals, Solon, OH), glucagon, and C-peptide by radioimmunoassay. Body composition was determined using Bruker Minispec NMR (Bruker Optics, The Woodlands, TX).

From the [1]Department of Medicine, Columbia University, New York, New York; the [2]Diabetes Research and Training Center, Albert Einstein College of Medicine, Bronx, New York; and the [3]Section of Comparative Medicine, Yale University School of Medicine, New Haven, Connecticut.

Corresponding author: Domenico Accili, da230@columbia.edu.

Received on 2 September 2009 and accepted 6 November 2009. Published ahead of print at http://diabetes.diabetesjournals.org on 23 November 2009. DOI: 10.2337/db09-1303.

Body weight and food intake. Body weight was measured weekly. Food intake was measured biweekly in 6- to 12-week-old mice using manual feeding hoppers. For refeeding studies, after acclimation mice were fasted overnight. Feeding hoppers were placed in the cages 2 h after the start of the light phase, and food intake was measured 6 h after feeding hoppers were placed.

Glucagon and stress response. For glucagon measurement, fasting was started 2 h after the onset of the light phase. After a 6-h fast, blood was drawn from the tail vein. One week later, mice were again fasted for 6 h, followed by an intraperitoneal insulin injection (0.75 units/kg). Blood glucose was measured immediately before insulin injection and at 30 and 60 min after the injection. Mice used for analyses of the stress response were familiarized with gentle handling for 6–8 weeks prior to the experiment. For determination of basal plasma corticosterone, blood was drawn from the tail 1–2 h after the start of the light phase.

Euglycemic-hyperinsulinemic clamp studies. Four groups of 14- to 16-week-old normoglycemic male mice were studied: wild type ($n = 8$), L1 ($n = 13$), Agrp-KI ($n = 8$), and Pomc-KI ($n = 7$). We performed euglycemic-hyperinsulinemic clamps in conscious, catheterized mice as described (10).

Indirect calorimetry. Indirect calorimetry was performed using a TSE LabMaster system (TSE Systems). Individually housed mice were acclimated to the respiratory chambers for 24–36 h prior to the experiment, and gas exchanges, locomotor activity, and food intake were measured every 14 min for 3–6 days.

RNA isolation and RT-PCR analyses. We extracted total RNA using RNeasy Mini Kit and RNase-Free DNase Set (Qiagen, Valencia, CA). Quantitative PCRs were performed in triplicate using a DNA Engine Opticon 2 System (Bio-Rad, Hercules, CA) and DyNAmo HS SYBR green Q-PCR kit (New England Biolabs, Ipswich, MA). Primer sequences are available upon request. Relative mRNA levels were normalized to 36B4 (for liver and hypothalamus) or Rps3 (for white adipose tissue).

Western blotting. We prepared detergent extract from liver and muscle as described (20) and probed the membranes with antibodies against phospho-Akt (Ser473), total Akt, phospho-Stat3 (Tyr705) (Cell Signaling, Danvers, MA), total Stat3, InsRβ (C-19), and β-actin (Santa Cruz Biotechnology, Santa Cruz, CA).

Green fluorescent protein immunohistochemistry. We perfused mice transcardially with PBS followed by formalin, fixed and dissected brains, equilibrated them in 30% sucrose, and froze them in OCT (Sakura, Torrance, CA). We used 30-μm–thick coronal sections for green fluorescent protein immunostaining on free-floating sections with a polyclonal rabbit antiserum (Molecular Probes/Invitrogen, Carlsbad, CA).

PIP3 measurements. Phosphatidylinositol 3,4,5-trisphosphate (PIP3) immunostaining was performed as previously described (21) using a fluorescein isothiocyanate–conjugated antibody (catalog no. Z-G345; Echelon Biosciences, Salt Lake City, UT), a horseradish peroxidase–conjugated fluorescein isothiocyanate antibody, and TSA fluorescein tyramide reagent pack (PerkinElmer, Waltham, MA). For quantitative analysis of PIP3 levels, three coronal sections of each mouse at approximately Bregma −1.3 mm, −1.4 mm, and −1.5 mm were examined. A total of 700–850 cells per mouse were examined as previously described (6). Results were quantified and expressed as percentage of ARC cells showing moderate to high PIP3 levels.

Synaptology. The hypothalamus was dissected from 15- to 17-week-old male mice, and cut in 50-μm vibratome sections that were processed and analyzed as described (22). Owing to significant nonhomogeneity of variance among groups, data were analyzed by one-way nonparametric ANOVA (Kruskal-Wallis), and Mann-Whitney U test was used to determine significance ($P < 0.05$).

Statistical methods. We analyzed data with one-way ANOVA followed by post hoc Bonferroni test using SPSS software.

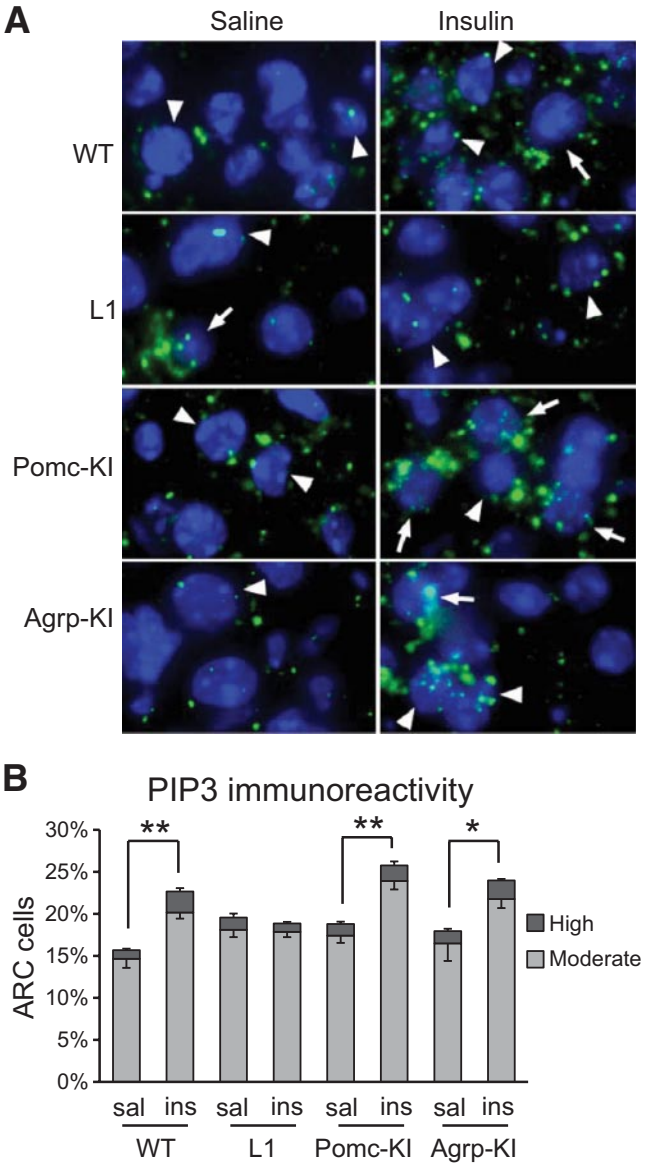

FIG. 1. PIP3 formation in ARC cells of wild-type, L1, Pomc-KI, and Agrp-KI mice. *A*: Immunohistochemistry of ARC sections of wild-type, L1, Pomc-KI, and Agrp-KI mice was performed in overnight-fasted animals, which were intravenously injected with either saline (*left panels*) or insulin (*right panels*) and killed 10 min after stimulation. Blue, DNA; green, PIP3. The amount of PIP3 was classified as high (arrows), moderate (arrowheads), or low as previously described (6). *B*: Quantification of ARC cells displaying moderate to high PIP3 levels in the basal state (sal) and after insulin stimulation (ins). $n = 4–6$ mice per group; 800–1,000 ARC cells per mouse were examined. Data are means ± SEM. *$P < 0.05$, **$P < 0.01$ saline versus insulin. (A high-quality digital representation of this figure is available in the online issue.)

RESULTS

Generation of Agrp-KI and Pomc-KI mice. To investigate the contribution of InsR signaling in AgRP and/or POMC neurons to insulin sensitivity and energy homeostasis, we reactivated InsR expression specifically in either of these neuron populations in L1 mice using a conditional locus knock-in approach (supplementary Fig. 1*A* and *B*, available in an online appendix at http://diabetes.diabetesjournals.org/cgi/content/full/db09-1303/DC1) (15). L1 mice in which Cre-mediated recombination resulted in InsR expression in AgRP or POMC neurons are denoted as Agrp knock-in (Agrp-KI) or Pomc knock-in (Pomc-KI), respectively. Cre-mediated recombination was assessed by intercrossing Cre transgenic lines with Rosa26-Gfp mice and revealed the expected expression patterns in ARC AgRP and POMC neurons (supplementary Fig. 1*C* and *D*), without affecting InsR levels in peripheral tissues (supplementary Fig. 1*E* and *F*).

To determine the effects of AgRP neuron– or POMC neuron–specific InsR reconstitution, we measured insulin's ability to activate the PI 3-kinase pathway in wild-type, L1, Agrp-KI, and Pomc-KI mice (21). In wild-type mice, we detected PIP3 immunoreactivity in 15.7% of ARC cells in the fasted state and in 22.5% of cells after insulin stimulation (Fig. 1*A* and *B*) ($P < 0.05$). Insulin failed to stimulate PIP3 formation in ARC of L1 mice (19.6 fasted

vs. 18.9% after insulin, respectively), but was effective in Pomc-KI mice (18.8 vs. 25.8%) and Agrp-KI (17.9 vs. 24.0%) mice, consistent with restoration of insulin/PI 3-kinase signaling in defined subpopulations of ARC neurons.

Opposite effects on insulin sensitivity in Agrp-KI and Pomc-KI mice. The expectation of the current study was that, by reconstituting InsR function in AgRP neurons or POMC neurons of L1 mice, insulin suppression of HGP would be restored. Consistent with previous reports (10,15), L1 mice showed hyperinsulinemia in the fasted and fed states, and 13% became diabetic by 12 weeks of age (Fig. 2*A* and *B*). Agrp-KI mice showed significant reductions in both fasted and fed insulin levels compared with L1, and only 9% were diabetic at 12 weeks. Pomc-KI mice showed insulin levels similar to L1 mice, but the frequency of diabetes nearly doubled to 23%. To circumvent potential secondary effects of chronic hyperglycemia on metabolism and energy homeostasis, we excluded diabetic L1, Agrp-KI, and Pomc-KI animals from further analyses. In intraperitoneal glucose tolerance tests, nondiabetic L1, Agrp-KI, and Pomc-KI mice displayed modest glucose intolerance compared with wild type (supplementary Fig. 2*A*), whereas insulin tolerance tests did not reveal differences among the four genotypes (supplementary Fig. 2*B*).

To accurately probe hepatic insulin sensitivity, we performed euglycemic hyperinsulinemic clamps in nondiabetic mice (Fig. 2*C–F*). Consistent with the results of glucose tolerance tests, rates of whole-body glucose disappearance in L1, Agrp-KI, and Pomc-KI mice were 10, 24, and 28% lower than wild type (Fig. 2*E*), respectively, indicating modest reductions in tissue glucose uptake. As previously described (10), the glucose infusion rate (GIR) required to maintain euglycemia was reduced by 36% and HGP was increased fourfold in L1 mice compared with wild type (Fig. 2*D* and *F*), consistent with hepatic insulin resistance. HGP was restored to normal in Agrp-KI mice, indicating that InsR in AgRP neurons is sufficient for insulin inhibition of HGP. In contrast, Pomc-KI mice exhibited a further 64% reduction in GIR and a 78% increase in HGP compared with L1, indicating a marked increase in hepatic insulin resistance.

This unexpected result prompted us to investigate the mechanism whereby InsR reconstitution in POMC neurons leads to a deterioration of hepatic insulin sensitivity. Changes in hepatic insulin signaling and counterregulatory responses failed to explain the phenotype (supplementary Figs. 3–6). We then explored two mutually nonexclusive hypotheses: *1*) altered regulation of genes involved in hypothalamic glucose sensing; and *2*) impaired neuropeptide regulation with attendant abnormalities of energy balance.

Reduced expression of hypothalamic K_{ATP} channels in Pomc-KI– and POMC-specific forkhead box class O knockout mice. Hypothalamic K_{ATP} channels link membrane excitability with cellular metabolism, and are regulated by glucose (23,24), insulin (25,26), and leptin (27). Cells in the mediobasal hypothalamus, including ~75% of POMC neurons, express the K_{ATP} channel sulfonylurea receptor 1 (SUR1) and Kir6.2 subunits (encoded by *Abcc8* and *Kcnj11*, respectively) (8,21,28). Activation of hypothalamic K_{ATP} channels lowers HGP, whereas SUR1 deficiency curtails insulin suppression of HGP (8). To determine whether abnormalities of K_{ATP} channel expression contribute to the increased HGP in Pomc-KI mice, we examined hypothalamic *Abcc8* and *Kcnj11* levels in fasted and in clamped mice. We detected a significant 43% reduction of *Abcc8* expression in clamped Pomc-KI mice compared with L1 and Agrp-KI mice (Fig. 3*A*), but no significant difference in *Kcnj11* among the four genotypes (Fig. 3*B*). The decrease of *Abcc8* is consistent with a reduction in insulin's ability to decrease neuronal firing, which in turn may contribute to increased HGP. (Fasted levels were also lower in Pomc-KI versus wild-type mice, but the difference failed to reach statistical significance.)

To further demonstrate that the observed reduction in *Abcc8* expression was linked to InsR signaling in POMC neurons, we measured hypothalamic *Abcc8* mRNA in mice lacking the insulin-regulated transcription factor forkhead box class O (FoxO1) in POMC neurons (*Foxo1*$^{\Delta POMC}$). The prediction was that *Foxo1*$^{\Delta POMC}$ mice should phenocopy the reduced Abcc8 levels of Pomc-KI mice. Indeed, we found a 53% decrease of Abcc8 in *Foxo1*$^{\Delta POMC}$ mice (Fig. 3*C*), consistent with our hypothesis that InsR signaling decreases *Abcc8* expression in POMC neurons.

Synaptic contacts in Pomc-KI mice. Owing to the complex genotype of Pomc-KI mice, we could not obtain primary neuronal cultures from newborns to perform electrophysiology. We thus performed a histomorphometric electron microscopy study of synaptic contacts, comparing wild-type, L1, and Pomc-KI mice. We found a significant decrease in the total number of synapses on POMC neurons of L1 and Pomc-KI mice that was entirely accounted for by decreased symmetric (putative inhibitory) contacts, whereas asymmetric (putative stimulatory) contacts were unchanged, resulting in increased ratios of asymmetric/symmetric contacts (Table 1). Pomc-KI mice had the lowest number of inhibitory contacts. This is consistent with the fact that, as insulin inhibits POMC neurons' electrical activity (21), these neurons are likely to recruit fewer inhibitory contacts from other cells. It stands to reason that the lack of inhibitory connections renders these neurons more excitable, leading to increased HGP (29).

Hypermetabolic state in Pomc-KI mice. We next explored the contribution of altered energy balance and hypothalamic neuropeptide expression to the impairment of hepatic insulin sensitivity in Pomc-KI mice. As weanlings, L1, Agrp-KI, and Pomc-KI showed a 30% reduction of body weight compared with wild-type mice, and exhibited limited catch-up growth thereafter, attaining ~90% of normal weight at 16 weeks of age (Fig. 4*A*). This was associated with a 25% decrease in plasma IGF-1 levels, and resulted in an 11% decrease of BMIs (supplementary Table 1). Most importantly, for the purpose of the ensuing studies, body composition of the four groups of mice was similar (supplementary Table 1).

In view of the melanocortinergic (MCR) effects of insulin in the hypothalamus (30), we predicted that energy expenditure in L1 mice would reflect decreased MCR signaling, and that AgRP and POMC knock-ins would partially restore MCR effects. As reported previously, L1 mice had similar food intake to wild type (10) (Fig. 4*B*), and exhibited normal oxygen consumption (V_{O_2}) and respiratory quotient (Fig. 4*C–F*). They also showed a marked decrease in locomotor activity during the dark phase of the light cycle (Fig. 4*G* and *H*). These data indicate that some MCR actions are preserved in L1 mice (food intake, V_{O_2}), whereas others are impaired (locomotor activity and suppression of HGP) (31,32). InsR reconstitution in AgRP neurons failed to normalize locomotor activity (Fig. 4*G* and *H*), but restored insulin suppression of HGP (Fig. 2). There was a modest increase in V_{O_2} during

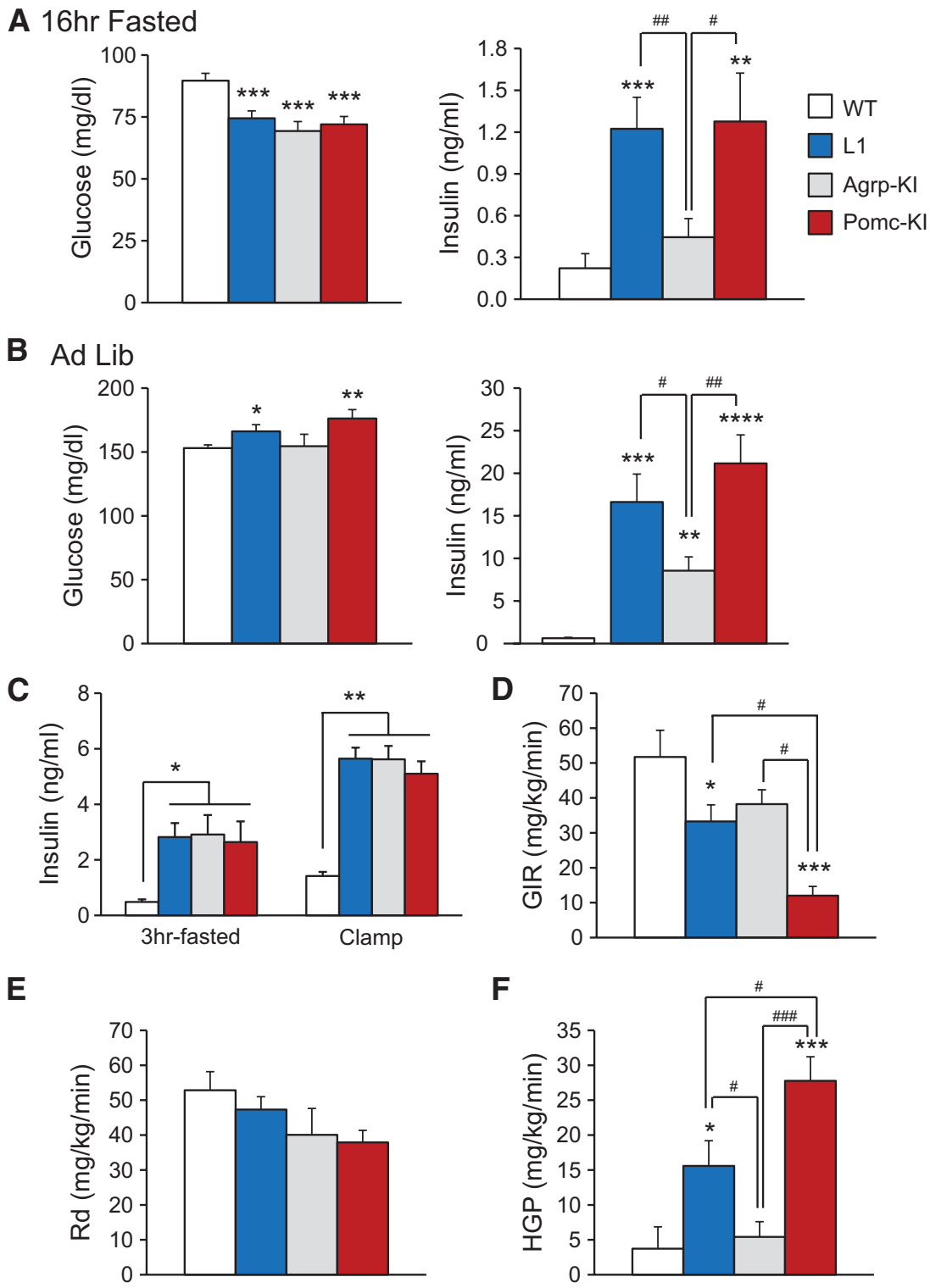

FIG. 2. Opposite effects on glucose homeostasis in Agrp-KI and Pomc-KI mice. *A* and *B*: Blood glucose levels (*left panels*) and plasma insulin levels (*right panels*) in overnight-fasted (*A*) and ad libitum–fed (*B*) 12- to 14-week-old wild-type, L1, Agrp-KI, and Pomc-KI males (n = 11–80). *C*: Plasma insulin levels in 14- to 16-week-old, 3-h–fasted wild-type, L1, Agrp-KI, and Pomc-KI male mice before the hyperinsulinemic-euglycemic clamp protocol (0 min) and during the steady state (mean of 60 and 90 min) of the clamps. *D–F*: GIRs (*D*), rates of whole-body glucose disappearance (Rd) (*E*), and HGP during the steady state of the clamp studies (*F*) (n = 8 for wild type, n = 12 for L1, n = 8 for Agrp-KI, and n = 7 for Pomc-KI). All values are means ± SEM. *P < 0.05 versus wild type, **P < 0.01 versus wild type, ***P < 0.001 versus wild type, ****P < 0.0001 versus wild type, #P < 0.05, ##P < 0.01, ###P < 0.001.

the light phase and no changes in other parameters (Fig. 4*B–F*). Reconstitution of InsR in POMC neurons completely reversed the decrease in locomotor activity in L1 mice (Fig. 4*G–H*) and increased V_{O_2} (Fig. 4*C* and *D*).

AgRP and POMC neurons project to the lateral hypothalamus, the site of melanin-concentrating hormone (*Mch*)– or hypocretin (*Hcrt*)–expressing neurons (33,34) that have been implicated in the regulation of locomotor

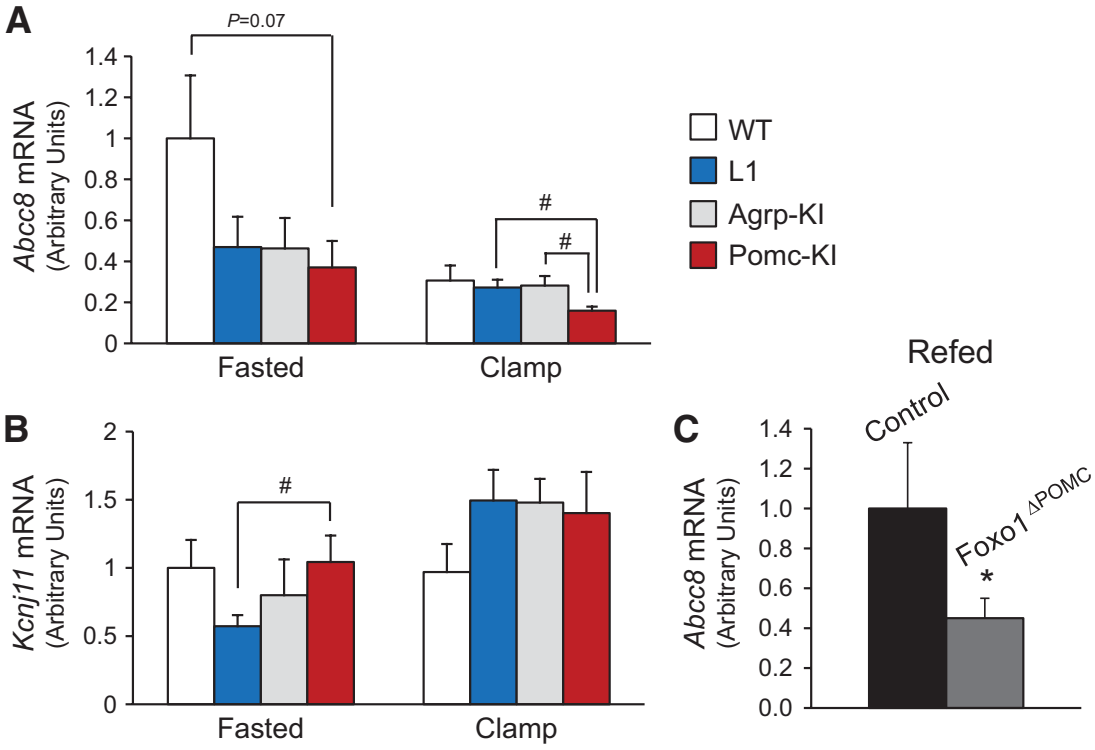

FIG. 3. Hypothalamic expression of K_{ATP} channel subunits. *A* and *B*: mRNA expression of *Abcc8* and *Kcnj11* quantified by real-time RT-PCR in whole hypothalamic lysates of 14- to 16-week-old wild-type, L1, Agrp-KI, and Pomc-KI male mice after overnight fasting or at the end of hyperinsulinemic-euglycemic clamps (n = 7–12). *C*: mRNA expression of *Abcc8* in whole hypothalamic lysates of 15-week-old *Foxo1*$^{flox/flox}$ (control) and *Foxo1*$^{flox/flox}$*::Pomc-Cre* (*Foxo1*$^{\Delta POMC}$) male mice after 16-h fasting/6-h refeeding (n = 6). All values are means ± SEM. *$P < 0.05$ versus wild type, #$P < 0.05$.

activity (35,36). Fasting *Mch* and *Hcrt* levels were similar in all genotypes (supplementary Fig. 7). Under hyperinsulinemic clamp conditions, expression of *Mch* and *Hcrt* tended to be elevated in L1, Agrp-KI, and Pomc-KI compared with wild type, but the differences were not statistically significant.

The hypermetabolic state of Pomc-KI mice, in the presence of normal body weight/composition, led us to investigate their food intake. Pomc-KI mice showed modest increases in ad libitum feeding (Fig. 4*B*) and a 36% increase in rebound food intake after fasting (Fig. 4*I*). This was associated with a 34–87% reduction in plasma leptin levels under ad libitum–fed, overnight-fasted, and 6-h–refed conditions compared with L1 mice (Fig. 4*J*) and a parallel reduction in leptin mRNA expression in adipose tissue (Fig. 4*K*). The dissociation of leptin's ability to modulate energy expenditure from regulation of food intake in Pomc-KI mice provides indirect evidence that MCR target neurons regulating energy expenditure are distinct from those regulating food intake (12).

TABLE 1
Synaptic contacts in L1 and Pomc-KI mice

Genotype	n	Asymmetric (stimulatory) contacts	Symmetric (inhibitory) contacts	Total synapses
WT	4	8 ± 2	15.33 ± 3.06	23.22 ± 3.98
L1	5	8.5 ± 1.5	6 ± 1.68*	14.5 ± 2.11*
Pomc-KI	5	12 ± 2.36	4 ± 1.33*	15 ± 3.03*

Data are connections/100 μ of perikaryal membrane. *$P < 0.05$ by Mann-Whitney U test.

We determined the ability of clamp-induced hyperinsulinemia to affect *Agrp* and *Pomc* expression by comparing mRNA levels of the respective genes in fasted and in clamped mice. Insulin infusion raised *Pomc* levels in wild-type mice (Fig. 5*A*); the effect was blunted in L1 and Agrp-KI, and normalized in Pomc-KI mice, consistent with cell-autonomous restoration of InsR-dependent *Pomc* activation. In contrast, *Agrp* levels were unaffected by clamp hyperinsulinemia in wild-type mice, probably reflecting different time course and dose sensitivity of insulin regulation of this gene. Nonetheless, in L1 mice we observed a trend toward insulin inhibition of *Agrp* that became statistically significant in both Agrp-KI and Pomc-KI mice (Fig. 5*B*). These data provide critical support for the mechanism proposed by Barsh and colleagues (37), according to which AgRP neurons are regulated by insulin in both a cell-autonomous manner (explaining *Agrp* inhibition in Agrp-KI mice) and a nonautonomous manner that includes POMC neurons (explaining *Agrp* inhibition in Pomc-KI mice) and other inhibitory postsynaptic neurons (explaining the trend toward lower *Agrp* levels in L1 mice).

In summary (Fig. 6), hypothalamic insulin signaling controls both glucose metabolism and energy balance. InsR signaling in AgRP neurons restrains HGP independent of energy expenditure, whereas one-sided InsR activation in POMC neurons results in increased HGP. In addition, Pomc-KI mice show increased energy expenditure without attendant hypophagia. The rebound hyperphagia in Pomc-KI mice is probably due to hypoleptinemia and lack of concurrent inhibition of anabolic AgRP neurons.

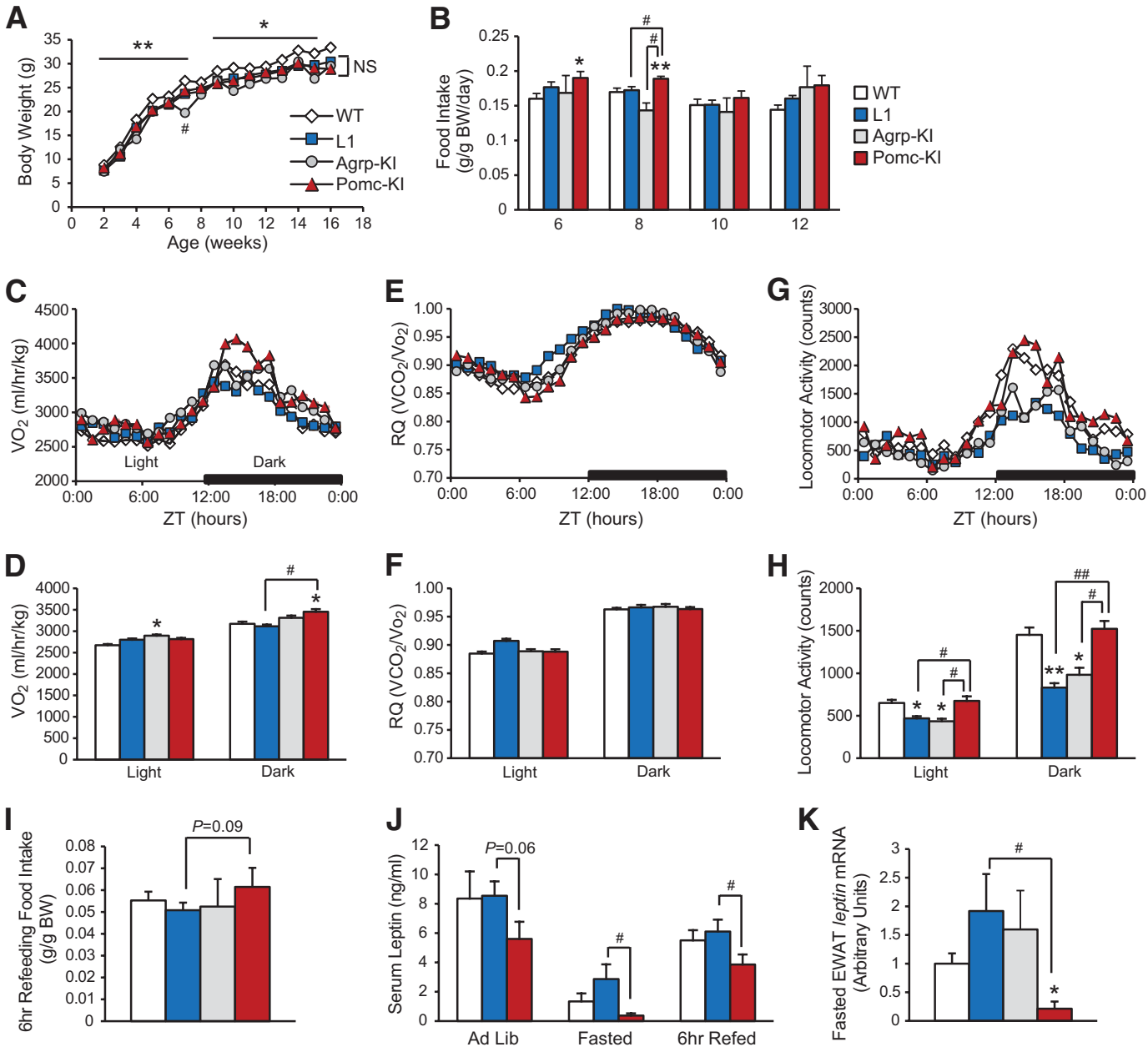

FIG. 4. Energy homeostasis in Agrp-KI and Pomc-KI mice. ***A*: Mean body weight of 2- to 16-week-old male mice (n = 4–44). *P < 0.05 wild type versus L1, Agrp-KI, and Pomc-KI; **P < 0.01 wild type versus L1, Agrp-KI, and Pomc-KI; #P < 0.001 Agrp-KI versus L1 and Pomc-KI; NS, not significant. *B*: Daily food intake of regular chow diet per gram of body weight (BW) of 6- to 12-week-old male mice (n = 4–37). *C–H*: Indirect calorimetry measurements in 12-week-old, weight-matched, nondiabetic male mice. *C*: Hourly averages of oxygen consumption. *E*: Respiratory quotient. *G*: Spontaneous locomotor activity. *D*, *F*, and *H*: Corresponding 12-h averages during light and dark phases. SE and statistical significance are omitted in *C*, *E*, and *G* for simplicity. Data in *D*, *F*, and *H* are means ± SEM (n = 4–8 mice and 19–31 days/mouse). *P < 0.05 versus wild type, **P < 0.01 versus wild type, #P < 0.05, ##P < 0.01. *I*: Six-hour food intake after a 16-h fast per gram of body weight in 13- to 15-week-old male mice (n = 5–23). *J*: Plasma leptin levels in ad libitum–fed, 16-h fasted, and 16-h fasted/6-h refed, 13- to 15-week-old mice (n = 7–25). *P < 0.05 versus wild type, #P < 0.05 L1 versus Pomc-KI. *K*: *leptin* mRNA expression in perigonadal fat pads of 14- to 17-week-old mice after overnight fasting. Data are normalized against *Rps3* mRNA (n = 4–8). *P < 0.05 versus wild type, #P < 0.05 versus L1.**

DISCUSSION

Our findings support a branched-pathway model of hypothalamic insulin action (Fig. 6). In essence, *1*) hypothalamic regulation of HGP by insulin appears to be a cell-autonomous response mediated by AgRP neurons; and *2*) regulation of locomotor activity and energy expenditure appears to occur in a cell-autonomous manner via POMC neurons. Based on the findings of Balthasar et al. (12), it can be inferred that this response is mediated by second-order MCR neurons distinct from those in the paraventricular hypothalamus (PVH). Finally, *3*) the anorexigenic response to insulin appears to require direct coregulation of POMC and AgRP neurons, as suggested by Barsh and colleagues (37). The physiologic implication of the present work is that different subsets of neurons mediate the pleiotropic actions of insulin in the hypothalamus.

Mechanisms of increased HGP in Pomc-KI mice. The increase of HGP in Pomc-KI mice has three likely components: *1*) a modest increase in hepatic glucose-6-phosphatase expression; *2*) hypermetabolic state, acting perhaps to increase substrate flux to the liver (38); and *3*) decreased hypothalamic K_{ATP} channels. Insulin hyperpolar-

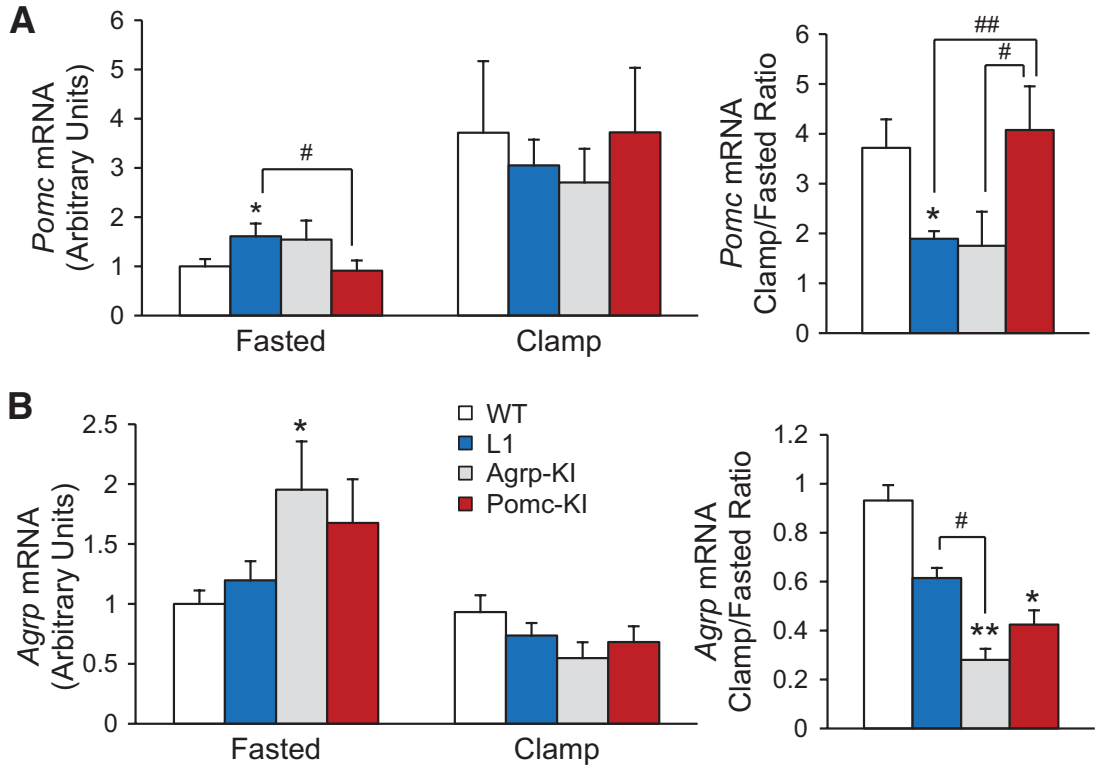

FIG. 5. Hypothalamic mRNA expression. *A* and *B*: *Pomc* and *Agrp* mRNA in 14- to 16-week-old wild-type, L1, Agrp-KI, and Pomc-KI male mice after overnight fasting or hyperinsulinemic clamp (*left panels*). Relative ratio between clamped and fasted mice was calculated (*right panels*). *n* = 6–11 per group. All values are means ± SEM. **P* < 0.05 versus wild type, ***P* < 0.01 versus wild type, #*P* < 0.05, ##*P* < 0.01. Data are normalized by *36B4* mRNA.

izes AgRP (11) and POMC neurons (21,26) through activation of K_{ATP} channels in the mediobasal hypothalamus that results in HGP inhibition (8,9). The complex genetic makeup of Agrp-KI and Pomc-KI mice precludes direct electrophysiological studies. But *Abcc8* expression was significantly lower in Pomc-KI mice than in any other genotype during hyperinsulinemic clamps. It should be noted that *Abcc8* mRNA levels mirror SUR1 protein levels (39). Thus, decreased *Abcc8* correlates with insulin's failure to inhibit HGP, and suggests that hypothalamic neurons are constitutively depolarized in these mice, and therefore resistant to insulin inhibition of their electrical activity. Further evidence that the decrease of *Abcc8* is linked to InsR knock-in is provided by the observation that FoxO1 ablation in POMC neurons phenocopies this effect. Although the current data do not allow us to pinpoint the site of *Abcc8* reduction, the magnitude of the reduction suggests that, in addition to POMC neurons, *Abcc8* is also reduced in other arcuate cells, potentially including AgRP neurons, thereby increasing HGP. Together with the observation of decreased inhibitory synaptic contacts on POMC neurons in L1 mice, these data indicate that lack of InsR constitutively depolarizes hypothalamic neurons and that one-sided restoration of InsR signaling in Pomc-KI mice further decreases inhibitory synapses, presumably because it inhibits POMC neuron electrical activity, thus decreasing the need to recruit further inhibitory connections. The decrease of inhibitory contacts, in the presence of normal excitatory contacts, sets the stage for increased HGP. We also considered a potential contribution of neuropeptide alterations to increasing HGP, as intracerebroventricular infusion of α-melanocyte-stimulating hormone (αMSH), a processing product of POMC, was shown to acutely increase HGP (40). However, Pomc expression in Pomc-KI mice was unaltered during the hyperinsulinemic clamp, arguing against a significant change in αMSH. Future studies will be required to determine whether hyperinsulinemia affects αMSH release in Pomc-KI mice, thus contributing to increased HGP.

Our findings significantly expand upon a recent conditional knockout study demonstrating that InsR in AgRP neurons is necessary to suppress HGP (11). Our data go further, and indicate that InsR in AgRP neurons is sufficient to confer insulin inhibition on HGP. However, whereas IL-6 expression was decreased in liver of AgRP-specific InsR knockouts during hyperinsulinemic clamps, Agrp-KI mice showed no improvement in hepatic IL-6/Stat3 signaling compared with L1, possibly reflecting different duration of the fast prior to clamping (3–5 in this study vs. 16 h in the study by Könner et al. [11]). In contrast to our findings, conditional ablation of InsR in POMC neurons did not result in abnormalities of HGP (11). The likeliest explanation for this difference is that, under normal conditions and in the presence of concurrent activation of InsR in AgRP neurons, it would have been difficult to detect an increase in hepatic insulin sensitivity in Pomc-InsR knockouts. The data underscore the need to examine these complex questions using different models.

Diverging effects of InsR signaling on locomotor activity and feeding behavior. The reciprocal changes in locomotor activity observed in L1, Agrp-KI, and Pomc-KI provide evidence for a dominant role of hypothalamic InsR signaling in regulating this process. The hypothalamic effects of insulin on energy homeostasis are mediated primarily through the MCR system (32). Our data suggest that the locomotor/energy expenditure branch of

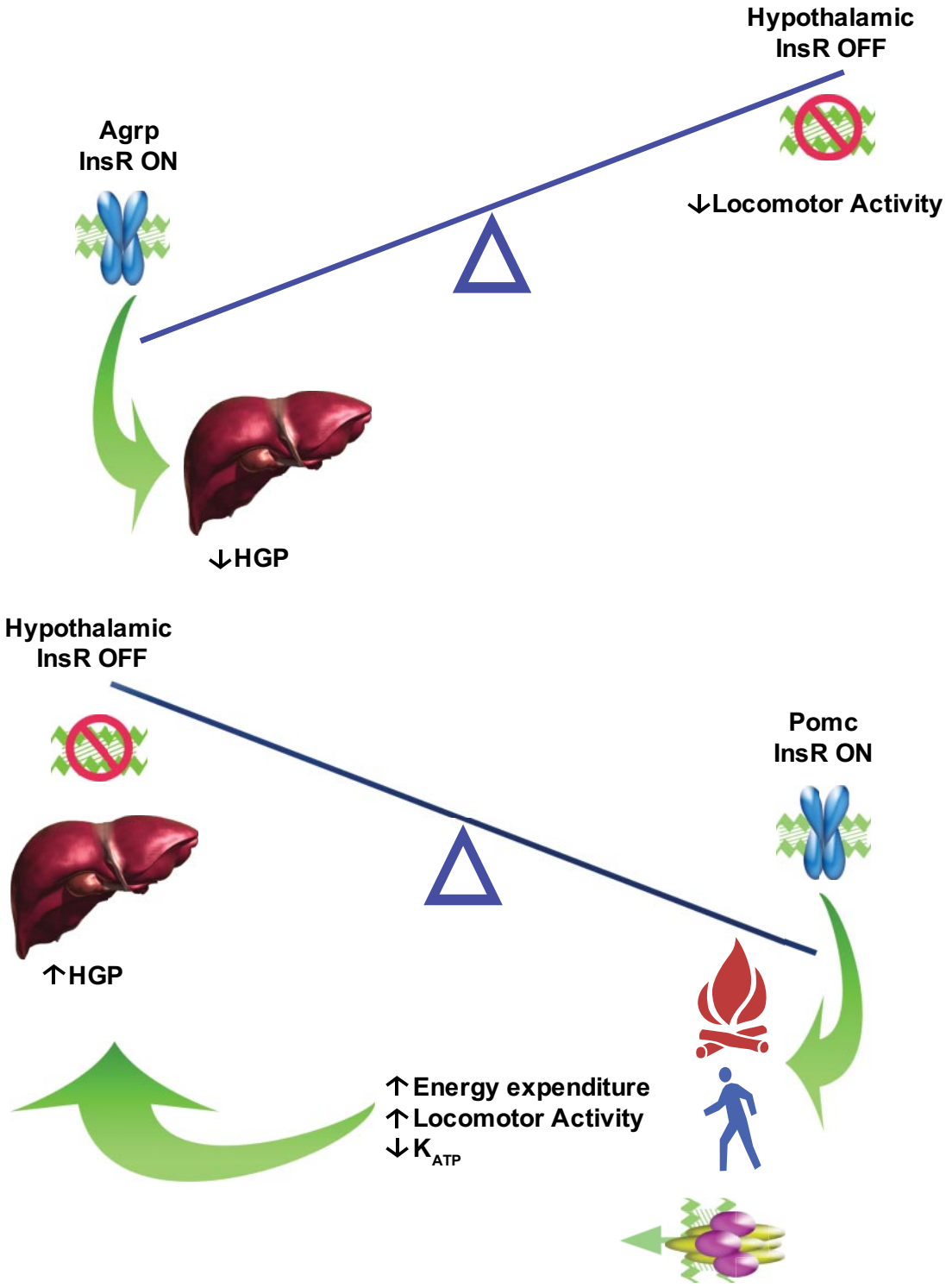

FIG. 6. Branched pathways in hypothalamic InsR action. InsR activation in AgRP neurons restrains HGP independent of locomotor activity/energy expenditure. In contrast, InsR activation in POMC neurons results in increased HGP (in part through downregulation of K_{ATP} channels and activation of a hypermetabolic state) and increased locomotor activity/energy expenditure.

MCR signaling is directly controlled via InsR signaling in POMC neurons, whereas the food intake branch of MCR signaling is largely unaffected by it. This is consistent with the demonstration that these two branches of MCR signaling are regulated by different neuronal subpopulations, with the PVH subset being more important for food intake (12). Accordingly, it can be inferred that InsR signaling is coupled primarily to POMC neurons that project to second-order MCR neurons distinct from those residing in the PVH. In addition to the PVH, ARC POMC neurons also project widely throughout the brain, including to the lateral hypothalamus, amygdala, and reticular nucleus (41). Lateral hypothalamus hypocretin and melanin-concentrating hormone neurons have been implicated in the regulation of energy expenditure, but we failed to detect differences in mRNA levels, indicating that the contribu-

tion of these pathways to the observed phenotype—if any—does not involve changes in gene expression. A recent study suggested that Stat3 signaling in AgRP neurons controls locomotor activity via secondary dopaminergic neurons in the striatum and frontal cortex (42). Further studies will be required to ascertain the contribution of POMC neurons in the nucleus of the solitary tract (41) and the role of secondary dopaminergic neurons to the observed phenotype.

The dissociation of InsR pathways regulating energy expenditure from those regulating food intake provides a likely explanation for the absence of obesity in the three models of hypothalamic insulin resistance presented in this article, unlike NIRKO mice (4). Although Pomc-KI mice show a trend toward increased rebound feeding, it should be considered that they are relatively hypoleptinemic. It bears emphasizing that Pten ablation in POMC neurons leads to hyperphagia and hyperleptinemia (21), consistent with the concept that the balance of hypothalamic InsR signaling is a key determinant of leptin production. The mechanism linking InsR hypothalamic signaling to leptin expression in adipocytes may involve nutritional and hormonal inputs and sympathetic nervous system cues (43). Hyperinsulinemia can induce sympathoactivation via PI 3-kinase and mitogen-activated protein kinase signaling in the rat mediobasal hypothalamus (44). It will be of interest to determine whether insulin action in POMC neurons regulates the sympathetic nervous system and contributes to the tonic inhibition of leptin production.

In conclusion, we demonstrate that different subsets of hypothalamic neurons mediate different branches of insulin's metabolic and energy expenditure actions. The data delineate an anatomic-functional map of hypothalamic insulin signaling that will be useful to interpret safety and efficacy data of antiobesity medications with a central mechanism of action.

ACKNOWLEDGMENTS

This work was supported by the Berrie Fellowship Award to H.V.L., Deutsche Forschungsgemeinschaft Grant PL542/1-1 to L.P., National Institutes of Health Grants DK-58282 and DK-57539 to D.A., the Columbia University Diabetes and Endocrinology Research Center (DK-63608), and the Einstein Diabetes Research and Training Center (DK-20541).

No potential conflicts of interest relevant to this article were reported.

Parts of this study were presented in abstract form at the 68th Scientific Sessions of the American Diabetes Association, San Francisco, California, 6–10 June 2008.

We thank B. Liu, K. Aizawa, Y. Su, R. Sgueglia, Q. Xu, Y. Dam, and B. Sarman for expert technical assistance and members of the Accili, Gutiérrez-Juárez, and Horvath laboratories for helpful discussion of the data.

REFERENCES

1. Havrankova J, Roth J, Brownstein M. Insulin receptors are widely distributed in the central nervous system of the rat. Nature 1978;272:827–829
2. Hill JM, Lesniak MA, Pert CB, Roth J. Autoradiographic localization of insulin receptors in rat brain: prominence in olfactory and limbic areas. Neuroscience 1986;17:1127–1138
3. Morton GJ, Cummings DE, Baskin DG, Barsh GS, Schwartz MW. Central nervous system control of food intake and body weight. Nature 2006;443:289–295
4. Brüning JC, Gautam D, Burks DJ, Gillette J, Schubert M, Orban PC, Klein R, Krone W, Müller-Wieland D, Kahn CR. Role of brain insulin receptor in control of body weight and reproduction. Science 2000;289:2122–2155
5. Woods SC, Lotter EC, McKay LD, Porte D Jr. Chronic intracerebroventricular infusion of insulin reduces food intake and body weight of baboons. Nature 1979;282:503–505
6. Plum L, Belgardt BF, Brüning JC. Central insulin action in energy and glucose homeostasis. J Clin Invest 2006;116:1761–1766
7. McGowan MK, Andrews KM, Fenner D, Grossman SP. Chronic intrahypothalamic insulin infusion in the rat: behavioral specificity. Physiol Behav 1993;54:1031–1034
8. Pocai A, Lam TK, Gutierrez-Juarez R, Obici S, Schwartz GJ, Bryan J, Aguilar-Bryan L, Rossetti L. Hypothalamic K(ATP) channels control hepatic glucose production. Nature 2005;434:1026–1031
9. Obici S, Feng Z, Karkanias G, Baskin DG, Rossetti L. Decreasing hypothalamic insulin receptors causes hyperphagia and insulin resistance in rats. Nat Neurosci 2002;5:566–572
10. Okamoto H, Obici S, Accili D, Rossetti L. Restoration of liver insulin signaling in Insr knockout mice fails to normalize hepatic insulin action. J Clin Invest 2005;115:1314–1322
11. Könner AC, Janoschek R, Plum L, Jordan SD, Rother E, Ma X, Xu C, Enriori P, Hampel B, Barsh GS, Kahn CR, Cowley MA, Ashcroft FM, Brüning JC. Insulin action in AgRP-expressing neurons is required for suppression of hepatic glucose production. Cell Metab 2007;5:438–449
12. Balthasar N, Dalgaard LT, Lee CE, Yu J, Funahashi H, Williams T, Ferreira M, Tang V, McGovern RA, Kenny CD, Christiansen LM, Edelstein E, Choi B, Boss O, Aschkenasi C, Zhang CY, Mountjoy K, Kishi T, Elmquist JK, Lowell BB. Divergence of melanocortin pathways in the control of food intake and energy expenditure. Cell 2005;123:493–505
13. Bates SH, Stearns WH, Dundon TA, Schubert M, Tso AW, Wang Y, Banks AS, Lavery HJ, Haq AK, Maratos-Flier E, Neel BG, Schwartz MW, Myers MG Jr. STAT3 signalling is required for leptin regulation of energy balance but not reproduction. Nature 2003;421:856–859
14. Accili D, Drago J, Lee EJ, Johnson MD, Cool MH, Salvatore P, Asico LD, José PA, Taylor SI, Westphal H. Early neonatal death in mice homozygous for a null allele of the insulin receptor gene. Nat Genet 1996;12:106–109
15. Okamoto H, Nakae J, Kitamura T, Park BC, Dragatsis I, Accili D. Transgenic rescue of insulin receptor-deficient mice. J Clin Invest 2004;114:214–223
16. Matsumoto M, Pocai A, Rossetti L, Depinho RA, Accili D. Impaired regulation of hepatic glucose production in mice lacking the forkhead transcription factor Foxo1 in liver. Cell Metab 2007;6:208–216
17. Kaelin CB, Xu AW, Lu XY, Barsh GS. Transcriptional regulation of agouti-related protein (Agrp) in transgenic mice. Endocrinology 2004;145:5798–5806
18. Balthasar N, Coppari R, McMinn J, Liu SM, Lee CE, Tang V, Kenny CD, McGovern RA, Chua SC Jr, Elmquist JK, Lowell BB. Leptin receptor signaling in POMC neurons is required for normal body weight homeostasis. Neuron 2004;42:983–991
19. Lin HV, Kim JY, Pocai A, Rossetti L, Shapiro L, Scherer PE, Accili D. Adiponectin resistance exacerbates insulin resistance in insulin receptor transgenic/knockout mice. Diabetes 2007;56:1969–1976
20. Kido Y, Burks DJ, Withers D, Bruning JC, Kahn CR, White MF, Accili D. Tissue-specific insulin resistance in mice with mutations in the insulin receptor, IRS-1, and IRS-2. J Clin Invest 2000;105:199–205
21. Plum L, Ma X, Hampel B, Balthasar N, Coppari R, Münzberg H, Shanabrough M, Burdakov D, Rother E, Janoschek R, Alber J, Belgardt BF, Koch L, Seibler J, Schwenk F, Fekete C, Suzuki A, Mak TW, Krone W, Horvath TL, Ashcroft FM, Brüning JC. Enhanced PIP3 signaling in POMC neurons causes KATP channel activation and leads to diet-sensitive obesity. J Clin Invest 2006;116:1886–1901
22. Parducz A, Zsarnovszky A, Naftolin F, Horvath TL. Estradiol affects axo-somatic contacts of neuroendocrine cells in the arcuate nucleus of adult rats. Neuroscience 2003;117:791–794
23. Ashford ML, Boden PR, Treherne JM. Glucose-induced excitation of hypothalamic neurones is mediated by ATP-sensitive K+ channels. Pflugers Arch 1990;415:479–483
24. Miki T, Liss B, Minami K, Shiuchi T, Saraya A, Kashima Y, Horiuchi M, Ashcroft F, Minokoshi Y, Roeper J, Seino S. ATP-sensitive K+ channels in the hypothalamus are essential for the maintenance of glucose homeostasis. Nat Neurosci 2001;4:507–512
25. Spanswick D, Smith MA, Mirshamsi S, Routh VH, Ashford ML. Insulin activates ATP-sensitive K+ channels in hypothalamic neurons of lean, but not obese rats. Nat Neurosci 2000;3:757–758
26. Choudhury AI, Heffron H, Smith MA, Al-Qassab H, Xu AW, Selman C, Simmgen M, Clements M, Claret M, Maccoll G, Bedford DC, Hisadome K, Diakonov I, Moosajee V, Bell JD, Speakman JR, Batterham RL, Barsh GS,

Ashford ML, Withers DJ. The role of insulin receptor substrate 2 in hypothalamic and beta cell function. J Clin Invest 2005;115:940–950
27. Spanswick D, Smith MA, Groppi VE, Logan SD, Ashford ML. Leptin inhibits hypothalamic neurons by activation of ATP-sensitive potassium channels. Nature 1997;390:521–525
28. Ibrahim N, Bosch MA, Smart JL, Qiu J, Rubinstein M, Rønnekleiv OK, Low MJ, Kelly MJ. Hypothalamic proopiomelanocortin neurons are glucose responsive and express K(ATP) channels. Endocrinology 2003;144:1331–1340
29. Parton LE, Ye CP, Coppari R, Enriori PJ, Choi B, Zhang CY, Xu C, Vianna CR, Balthasar N, Lee CE, Elmquist JK, Cowley MA, Lowell BB. Glucose sensing by POMC neurons regulates glucose homeostasis and is impaired in obesity. Nature 2007;449:228–232
30. Benoit SC, Air EL, Coolen LM, Strauss R, Jackman A, Clegg DJ, Seeley RJ, Woods SC. The catabolic action of insulin in the brain is mediated by melanocortins. J Neurosci 2002;22:9048–9052
31. Adage T, Scheurink AJ, de Boer SF, de Vries K, Konsman JP, Kuipers F, Adan RA, Baskin DG, Schwartz MW, van Dijk G. Hypothalamic, metabolic, and behavioral responses to pharmacological inhibition of CNS melanocortin signaling in rats. J Neurosci 2001;21:3639–3645
32. Obici S, Feng Z, Tan J, Liu L, Karkanias G, Rossetti L. Central melanocortin receptors regulate insulin action. J Clin Invest 2001;108:1079–1085
33. Broberger C, De Lecea L, Sutcliffe JG, Hökfelt T. Hypocretin/orexin- and melanin-concentrating hormone-expressing cells form distinct populations in the rodent lateral hypothalamus: relationship to the neuropeptide Y and agouti gene-related protein systems. J Comp Neurol 1998;402:460–474
34. Elias CF, Aschkenasi C, Lee C, Kelly J, Ahima RS, Bjorbaek C, Flier JS, Saper CB, Elmquist JK. Leptin differentially regulates NPY and POMC neurons projecting to the lateral hypothalamic area. Neuron 1999;23:775–786
35. Hagan MM, Rushing PA, Schwartz MW, Yagaloff KA, Burn P, Woods SC, Seeley RJ. Role of the CNS melanocortin system in the response to overfeeding. J Neurosci 1999;19:2362–2367
36. Segal-Lieberman G, Bradley RL, Kokkotou E, Carlson M, Trombly DJ, Wang X, Bates S, Myers MG Jr, Flier JS, Maratos-Flier E. Melanin-concentrating hormone is a critical mediator of the leptin-deficient phenotype. Proc Natl Acad Sci U S A 2003;100:10085–10090
37. Xu AW, Kaelin CB, Takeda K, Akira S, Schwartz MW, Barsh GS. PI3K integrates the action of insulin and leptin on hypothalamic neurons. J Clin Invest 2005;115:951–958
38. Obici S, Feng Z, Arduini A, Conti R, Rossetti L. Inhibition of hypothalamic carnitine palmitoyltransferase-1 decreases food intake and glucose production. Nat Med 2003;9:756–761
39. Hernández-Sánchez C, Ito Y, Ferrer J, Reitman M, LeRoith D. Characterization of the mouse sulfonylurea receptor 1 promoter and its regulation. J Biol Chem 1999;274:18261–18270
40. Gutiérrez-Juárez R, Obici S, Rossetti L. Melanocortin-independent effects of leptin on hepatic glucose fluxes. J Biol Chem 2004;279:49704–49715
41. Cone RD. Anatomy and regulation of the central melanocortin system. Nat Neurosci 2005;8:571–578
42. Mesaros A, Koralov SB, Rother E, Wunderlich FT, Ernst MB, Barsh GS, Rajewsky K, Brüning JC. Activation of Stat3 signaling in AgRP neurons promotes locomotor activity. Cell Metab 2008;7:236–248
43. Coll AP, Farooqi IS, O'Rahilly S. The hormonal control of food intake. Cell 2007;129:251–262
44. Rahmouni K, Morgan DA, Morgan GM, Liu X, Sigmund CD, Mark AL, Haynes WG. Hypothalamic PI3K and MAPK differentially mediate regional sympathetic activation to insulin. J Clin Invest 2004;114:652–658